

# Advances in Cesium Dispenser Photocathodes: Modeling and Experiment

**E. J. Montgomery,\* D. W. Feldman,† P. G. O'Shea,‡ Z. Pan,  
and N. Sennett**

*Institute for Research in Electronics and Applied Physics, University of Maryland,  
College Park, Maryland 20742*

**K. L. Jensen§**

*Vacuum Electronics Branch, Code 6843, ESTD, Naval Research Laboratory,  
Washington, D.C. 20375-5347*

**and**

**N. A. Moody¶**

*Los Alamos National Laboratory, TA-53, MSH851, Los Alamos, New Mexico 87545*

*Photocathodes are critical to the design of electron sources in high-power free-electron lasers but must maintain operational readiness and reliability with a long lifetime despite requisite high current density (hence high quantum efficiency), possible drive laser heating, and vacuum contamination. We at the University of Maryland have already demonstrated extended lifetime of cesiated metal photocathodes via the application of the dispenser cathode concept, a mature thermionic cathode technology, as part of our ongoing effort to develop the controlled porosity dispenser photocathode (CPD). This effort is now being extended to high-quantum-efficiency semiconductor coatings. The most efficient semiconductor coatings, notably those responsive to visible wavelengths (e.g., alkali antimonides), are prone to cesium loss in harsh operating environments; the dispenser concept promises in situ rejuvenation of cesiated surface layers by gently heating the cathode and allowing cesium to diffuse controllably to the surface through a porous substrate from a subsurface reservoir. Photocathode lifetime and robustness can be significantly enhanced. Essential to the advancement of the high-quantum-efficiency semiconductor, CPD is a comprehensive understanding of cesium's behavior. We here discuss the use of cesium in dispenser photocathodes in three photoemission topics: lower temperature operation of a modified cesium dispenser; development of a model for the diffusion of cesium on the surface of such a dispenser; and fabrication of cesium-based semiconductor coatings on the dispenser surface (cesium antimonide;  $Cs_3Sb$ ) for increased quantum efficiency.*

---

Received May 29, 2008; revision received September 15, 2008.

\*Corresponding author; e-mail: ejm1@umd.edu.

†E-mail: dfeldman@glue.umd.edu.

‡E-mail: poshea@umd.edu.

§E-mail: kevin.jensen@nrl.navy.mil.

¶E-mail: nmoody@lanl.gov.

**KEYWORDS:** Alkali antimonides, Cesium, Diffusion, Dispenser photocathode, Free-electron laser

## Nomenclature

$c$	speed of light
$D_o$	diffusion coefficient (alternately, <i>diffusivity</i> )
$F$	applied electric field strength at cathode, scaled units
$F_\lambda$	fraction of electrons reaching cathode surface after absorbing photons
$\hbar$	Planck's constant
$I$	photocurrent between anode and cathode
$j$	integer index (designating either pore number or spatial coordinate)
$k$	integer index (designating time coordinate)
$k_B$	Boltzmann's constant
$\mathbf{M}$	matrix representation of finite difference version of diffusion operator
$P$	drive laser power
$q$	electron charge
$R$	optical reflectivity of cathode surface
$r$	dimensionless ratio of spatial and temporal discretization terms with $D_o$
$T$	cathode surface temperature
$t$	time coordinate
$t_o$	initial time parameter governing spatial extent of initial unit cell diffusion
$U$	Fowler–Dubridge function
$u$	characteristic solution to diffusion equation
$x$	spatial coordinate on two-dimensional (2D) surface
$y$	spatial coordinate on 2D surface
$\Delta t$	temporal discretization parameter
$\Delta x$	spatial discretization parameter
$\Delta\theta_j$	$j$ th pore coverage coefficient
$\theta(x, y, t)$	local cesium coating thickness expressed as percent of one monolayer
$\lambda$	drive laser wavelength
$\mu$	chemical potential
$\phi$	cathode work function
$\tau$	characteristic evaporation time for coatings
$\tau_p$	characteristic resupply time for coatings from pores
$\omega$	drive laser angular frequency

## 1. Introduction

Laser-switched photoinjection, widely employed for prebunched electron beams in applications such as radio frequency (RF) linacs, free-electron lasers (FELs), and other accelerators,<sup>15</sup> commonly utilizes cesium-based photocathodes as the source of a high-quality electron beam. For the development of FELs in particular, increases in output optical power and commensurate increases in electron beam current place increasingly stringent requirements on the photocathode. In such high-power machines, the electron beam pushes the state of the art in current density, emittance, temporal structure, etc.<sup>9</sup> The effect on the cathode is to require efficient, prompt, robust, and long-lived emission. Efficiency must be

high to maximize the electrons emitted per incident drive laser pulse because drive laser power is limited by, if nothing else, power stability concerns in higher harmonic generation [i.e., frequency-doubled or -tripled yttrium–aluminum–garnet/yttrium–lithium–fluoride (YAG/YLF) lasers]. Promptness is required in the case of a representative RF accelerator operating at tens of gigahertz such that the electron pulse is a small fraction of the temporal period of the RF drive field: the electron pulse should be on the order of a few picoseconds. Robustness in the face of the harsh vacuum environment of a photoinjector-driven accelerator is essential, as is extended cathode lifetime, both to enhance operational readiness and to minimize complex maintenance procedures and downtime. These parameters are particularly critical for future high-power FELs: >3% quantum efficiency (QE) at green wavelengths, picosecond response time, and kilohour lifetime without unduly frequent reconditioning or rehabilitation.<sup>7,15</sup>

However, significant engineering and physics challenges must be overcome in the search for photocathodes meeting the above requirements, for the requirements are conflicting. No modern cathode simultaneously satisfies them all. Semiconductor coatings, being tens of nanometers thin, are prompt emitters. They can also achieve, as exemplified by the alkali antimonides, high QE at visible wavelengths, as can bulk crystalline semiconductors such as cesiated gallium arsenide (GaAs). For instance, potassium cesium antimonide ( $K_2CsSb$ ) has been shown to have  $QE > 8\%$  at 532 nm,<sup>13</sup> and cesiated GaAs can achieve  $QE > 10\%$  at green wavelengths.<sup>16</sup> In contrast to their high efficiency, the lifetime for the alkali antimonides is notoriously low, often merely hours in the environment of a working photoinjector, and their robustness is decreased by sensitivity to certain contaminant gases such as carbon dioxide and oxygen.<sup>2</sup> Alkali tellurides are longer-lived and more robust but have poor QE ( $<0.01\%$ )<sup>20</sup> at the ideal drive laser wavelengths in the green portion of the spectrum and thus are not suitable for high-power FEL applications due to drive laser shortcomings.

Short lifetime in cesium-based photocathodes is often attributed to loss of cesium<sup>19</sup> because the surface coatings are very delicate and susceptible to evaporation, backbombardment (in dc guns), and contamination (occupation of surface sites by high-work-function adatoms rather than alkali metals). The dispenser photocathode concept makes possible in situ rejuvenation of cesium-based coatings under gentle heating of the cathode, causing cesium to diffuse from the subsurface reservoir through a porous diffusion barrier and onto the photoemissive surface.

The development of a rugged, self-rejuvenating photocathode requires several coordinated experimental and theoretical efforts to determine the efficacy of the concept: evidence for both the rejuvenation of the surface as well as its final uniformity must be addressed, as both high QE and low emittance are required. Therefore, the program we report on contains elements to address these issues, all of which are built on a comprehensive understanding of the behavior of cesium in a dispenser photocathode. The three aspects we here report are, first, an experimental effort to reduce the operating temperature of a cesium dispenser using thinner diffusion barriers and improved cesium reservoir materials; second, development of a model for the diffusion of cesium on the surface of such a dispenser; and third, fabrication of cesium antimonide on the porous tungsten dispenser surface while testing QE as it is affected by cathode temperature, both to show increased QE and to probe the effects of heating on the cesium-based surface coating. We preface these three topics with a brief theoretical background of QE modeling and a description of our experimental apparatus and technique.

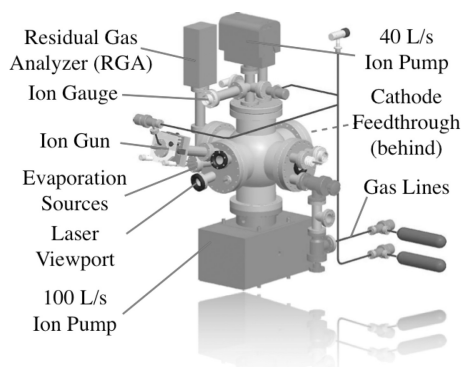


**Fig. 1.** Experimental apparatus.

## 2. Theoretical Background

A figure of merit of a photocathode is the number of electrons emitted compared to the number of incident photons of a given wavelength of light, designated the QE. Characterizing dispenser photocathodes primarily involves measuring the QE of selected coatings under a range of operating conditions, such as varying temperature, varying applied field, or background gas composition. The theoretical prediction of QE is involved, relating disparate phenomena such as reflectivity, laser penetration depth, relaxation rates, and temperature<sup>8</sup> that are beyond the present discussion, though the principal factors that determine QE are captured by a simpler “modified Fowler–Dubridge” model in which QE is given by<sup>6</sup>

$$\text{QE} = \left( \frac{q}{\hbar\omega} \right) \frac{J_{\lambda}(T, F, \Phi)}{I_{\lambda}(t)} \approx F_{\lambda}(T)(1 - R) \left\{ \frac{U[\beta_T(\hbar\omega - \phi)]}{U[\beta_T\mu]} \right\}, \quad (1)$$

where QE is the quantum efficiency of the cathode,  $I$  is the measured photocurrent between anode and cathode,  $F_{\lambda}$  is a scattering factor accounting for the loss of photoexcited electrons propagating to the cathode surface,  $R$  is the wavelength-dependent reflectivity of the surface,  $\lambda$  is the laser wavelength, and  $\beta_T$  is the inverse temperature  $1/k_B T$  in units of inverse energy. The usage of current density and laser intensity in Eq. (1) implicitly presumes that the temporal profile of the emitted current matches that of the incident laser, which for photon energies in excess of the work function for metals is generally the case. Under such conditions, when  $\lambda$  is given in nanometers,  $P$  in watts, and  $I$  in milliamperes, then Eq. (1) becomes

$$\text{QE} \approx \frac{I}{P} \frac{124}{\lambda}. \quad (2)$$

## 3. Experimental Apparatus

The experimental apparatus employed in this research is shown in Fig. 1. It consists of an ultrahigh vacuum chamber under 140-liter/s ion pumping, achieving pressures as low as  $3 \times 10^{-10}$  torr. The photocathode stem, consisting of a resistive ac heater coil (20 W max) and thermocouple beneath a cathode mount, allows gradual, controlled heating to temperatures for cesium diffusion of 150°–200°C or for dispenser activation of >500°C and orients the face of the dispenser cell horizontally. In front of the cathode is an annular anode, allowing

laser light to be directed at the cathode while applying fields of 5–30 kV/m. Beside the dispenser cell and facing the same direction is a quartz crystal deposition monitor with 0.1-Å precision to monitor thickness of deposited films (e.g., Sb, Cs, K). On the opposite side of the vacuum chamber are three ports. One allows video monitoring of the cathode and laser spots on its surface. A second has electrical feedthroughs for evaporative sources of Sb, Cs, K, and Na. The third is a quartz window for laser input. Outside this window, five low-power diode lasers are mounted on a translational stage. (Lower optical power enables electron extraction well below the Child–Langmuir limit<sup>17</sup> at the electric fields described such that the effect of space charge is minimal and the measurement of QE is accurate.) The lasers are automated to move to the window in turn, enabling measurement of photocurrent—hence QE—at the five laser wavelengths of 375, 405, 532, 655, and 808 nm. All automation and data collection is handled by LabVIEW software.

The apparatus also includes an ion gun with argon gas supply, operating at 0–10 keV and 10–40 mA. The total delivered charge during a standard cleaning (approximately 45 min at 10 mA and 6.4 keV to a 1 cm<sup>2</sup> cathode) is 30 mC. Given that sputtering rates for cesium and antimony under these beam conditions are greater than 1,000 Å/min, 45 min would seem more than sufficient to clean the surface of even relatively thick ~1,000-Å semiconductor layers. Indeed it is, but additionally, the process of ion cleaning does serve to increase roughness at the nanometer scale<sup>22</sup> and therefore the sputtering rate may decrease to statistically unfavorable levels for the last few adatoms after repeated cleanings due to an increase in surface roughness and thus a corresponding decrease in allowed angles for the sputtered adatoms to leave the substrate. Because it is important to ensure known initial conditions prior to each new deposition of semiconductor material by achieving an atomically clean substrate, we argon clean beyond the minimum required to do so.

## 4. Dispenser Photocathode Development

### 4.1. Cesium metal dispenser photocathodes

Cesium-based dispenser photocathodes are based on thermionic dispenser cathodes, a mature technology utilizing a porous substrate either impregnated with a work-function-lowering element (e.g., Ba) or acting as a diffusion barrier between a reservoir and the surface of the cathode. In photocathodes, the operational temperature is <200° C rather than the 1,000° C commonly used for thermionic dispensers. For this reason, the work-function-lowering element of choice is cesium (the most electropositive element): at these more modest temperatures it does not present problematic evaporation rates to the extent that it would in a thermionic cathode. We have previously reported the first demonstration of a cesium-based dispenser photocathode utilizing a subsurface reservoir and porous sintered tungsten diffusion barrier at the University of Maryland (UMD).<sup>11</sup> As shown in Fig. 2, the photoemissive surface is polished sintered tungsten, which is in turn brazed to a stainless-steel cell containing a pellet or cartridge of Cs source material.

### 4.2. Improved reservoir materials and diffusion barriers

Activation of the dispenser, a one-time procedure, is required to release elemental cesium into the reservoir from the Cs source material. This is done in the first generation of dispenser Cs sources by raising the cathode cell temperature to that required to react the cesium chromate (Cs<sub>2</sub>CrO<sub>3</sub>) with titanium, at 475° C, or in the second generation of dispenser

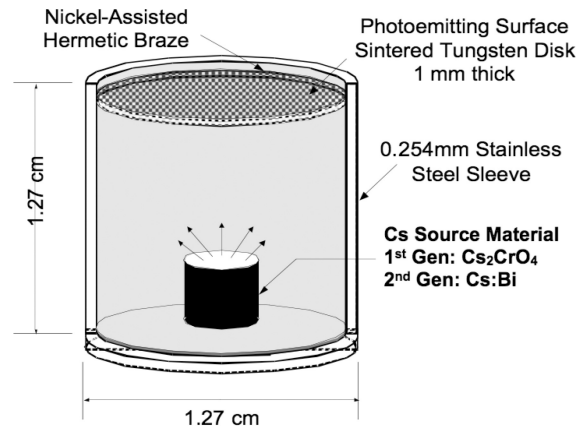


**Fig. 2.** Cutaway view of dispenser photocathode.

Cs sources to release free Cs from the Cs:Bi intermetallic compound, at 350° C. Once the dispenser has been activated, subsequent heatings at much lower temperatures are sufficient to cause Cs diffusion through the porous diffusion barrier and onto and across the surface.

To increase diffusion rates to the surface, the original 40-mil (1 mm) sintered tungsten barrier was replaced with a 20-mil (0.5 mm) barrier of identical 70% density. The minimum temperature at which cesium was seen diffusing onto the atomically clean tungsten surface on a timescale of a few hours (as indicated by an increase in QE from the bare-metal value through a characteristic peak at  $\theta = 67\%$ ) was reduced from 175° C to 135° C.

### 4.3. Lifetime and robustness

Dispensed Cs can be released in two operational modes: continuous or periodic. In particular, cathode lifetime in the continuous mode of operation has been compared to un-rejuvenated room-temperature lifetime. Results reported by our group elsewhere<sup>12</sup> indicate a remarkable 10-fold increase in the lifetime of the QE of a cesiated tungsten dispenser photocathode when using continuous rejuvenation mode.

## 5. Model Development for Cesium Diffusion in Dispenser Photocathodes

### 5.1. Motivation

Experimental results obtained through the UMD photocathode research program support parallel efforts in collaboration with the Naval Research Laboratory to develop physics-based, validated, predictive models of cesium diffusion and evaporation, photoemission from cesiated metals, and photoemission from semiconductor coatings such as the alkali antimonides. Photoemission models for semiconductor materials will be considered in a future work. Experimentally validated photoemission models for cesiated metals were published previously by Jensen et al.<sup>6,8</sup> We here consider the development of an initial model for cesium diffusion, a necessary prerequisite to understanding the supply of cesium to surface coatings (including alkali antimonide coatings) in dispenser photocathodes as well as the design of optimally porous diffusion barriers.

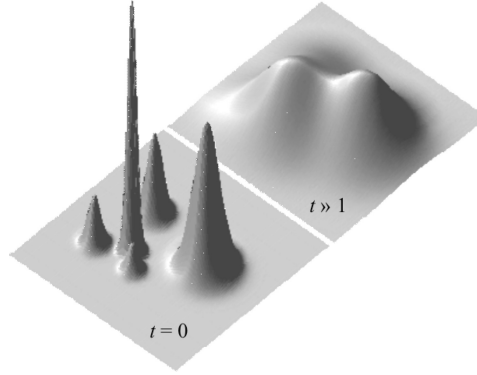


**Fig. 3.** Five-pore diffusion without resupply or evaporation.

## 5.2. Diffusion theory

Radial diffusion of cesium from a pore will follow Fick's law for the change of density (i.e., the relaxation of density fluctuations), as given by<sup>1</sup>

$$\partial_t \rho(\mathbf{r}, t) = \nabla \cdot [D_o \nabla \rho(\mathbf{r}, t)]. \quad (3)$$

We consider diffusion over a two-dimensional (2D) surface and equate the surface density to the fractional monolayer coverage factor  $\theta(x, y, t)$  under the assumption that  $D_o$  is approximately constant (though dependent on temperature). The behavior of a clump of cesium  $\Delta\theta_j$  exuded by a pore in a time increment  $\Delta t$  will add to previously exuded clumps and diffuse over the surface, as schematically illustrated in Fig. 3 for five such pores with differing  $\Delta\theta_j$  at an initial and a later time. Therefore, the contribution to the surface density of the  $j$ th pore due to time-integrated clumps from a single pore is described by

$$\theta_j(x, y, t) = \frac{\Delta\theta_j}{\Delta t} \int_0^t dt' \left( \frac{t_o}{t' + t_o} \right)^{-1/2} \exp \left[ -\frac{(x - x_j)^2 + (y - y_j)^2}{4D_o(t' + t_o)} \right], \quad (4)$$

where  $x_j$  and  $y_j$  are the coordinates of the center of the  $j$ th pore and  $t_o$  is such that the distribution at  $t = 0$  is comparable to the pore size. Usage of Eq. (4) in Eq. (3) with the aforementioned caveats results in the solution of an equation:

$$\partial_t u(x, y, t) = D_o(\partial_x^2 + \partial_y^2)u(x, y, t), \quad (5)$$

where  $u$  is a function from which  $\theta = \sum_j \theta_j$  is constructed. Stable and convergent *explicit* numerical schemes<sup>18</sup> for the solution of Eq. (5) require  $\Delta t \approx \Delta x^2/D_o$ , but this would create the potential for very small time steps if the spatial resolution is desired to be fine. Therefore an *implicit* numerical scheme that further allows predictor–corrector methods (as done for thermal equations<sup>6</sup>) needed for including evaporation will be used.

## 5.3. Numerical implementation

Letting the parameter  $r$  be given by  $r \equiv D_o \Delta t / \Delta x^2$  and using a second-order-accurate finite (central) difference scheme that creates a difference matrix  $\mathbf{M}$  that acts on a vector of values  $\theta(x, y) \rightarrow \theta[(i-1)\Delta x, (j-1)\Delta x] \Rightarrow \theta_{(i-1)N_x+j}$  and invoking periodic boundary

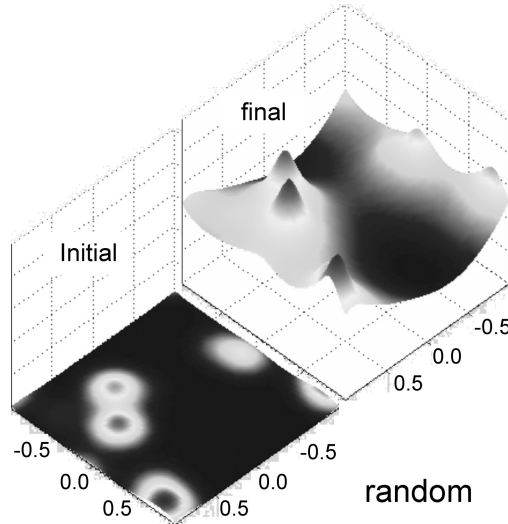


**Fig. 4.** Random porosity diffusion simulation including evaporation and resupply.

conditions, the implicit solution to Eq. (5) is given by (where the  $k$  superscript is the time index)

$$\theta^{k+1} = [\hat{I} - r\hat{M}]^{-1}[\hat{I} + r\hat{M}]\theta^k. \quad (6)$$

By virtue of being a 2D problem, the matrix  $\mathbf{M}$  is large; however, the matrix coefficient of  $\theta$  on the right-hand side of Eq. (6) need be evaluated only once and thereafter saved so long as the value of  $D_o$  remains constant and the discretization terms do not change.

Including evaporation and supply into Eq. (6) needs some finesse. The evaporation term requires an estimate of  $\theta^{k+1}$ , which is the quantity being sought by numerical evaluation. Under the assumption that the dispensation of Cs from the pore follows a prescribed time dependence, a prediction of  $\theta$  is made ( $\theta^*$ ) that is used to estimate  $\theta^{k+1}$ , and the process is iterated a number of times for convergence. Using a model of Cs evaporation<sup>14</sup> given by a power law ( $n$ ) dependence and a rate term  $\tau$ , we evaluate the discrete version of the evaporation + dispensation + diffusion equation

$$\theta^{k+1} = [\hat{I} - r\hat{M}]^{-1} [\hat{I} + r\hat{M}]\theta^k - \frac{\Delta t}{2\tau} [(\theta^*)^n + (\theta^k)^n] + \frac{\Delta t}{\tau_p} \delta\theta. \quad (7)$$

Two cases are considered: first, nine pores are assumed to be randomly distributed, as would occur in a conventional sintered tungsten dispenser cathode<sup>5</sup>; second, the pores are made uniform, as would occur in a controlled, porosity dispenser cathode.<sup>4,21</sup>

Figure 4 shows the initial (uncovered) surface and its final state after an arbitrary duration for a random pore surface, and, using the same conditions, Fig. 5 shows the same simulation for a uniform pore surface, for ad hoc values of the desorption and diffusion parameters nominally based on similar Ba on W terms under high temperature: it is known that the evaporation and pore diffusion times  $t$  and  $t_p$  are temperature dependent, so that the dominance of diffusion over evaporation, or vice versa, depends very much on operating conditions and is not a priori obvious. In a future work, simulations based on parameters

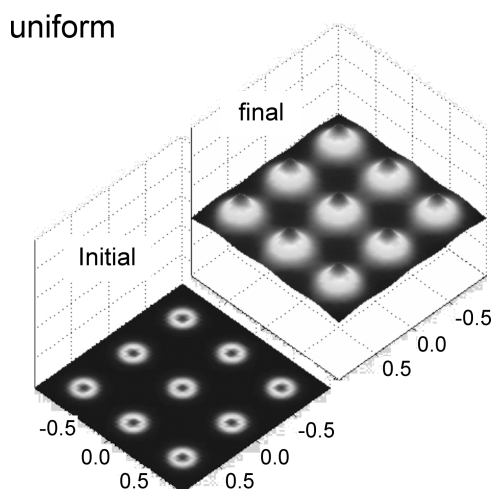


**Fig. 5.** Controlled porosity diffusion simulation including evaporation and resupply.

suggested from our ongoing experimental efforts to characterize quantities related to Cs on metal surfaces shall be considered.

Whereas the model described above applies generally to Cs diffusing on and evaporating from metal surfaces, the case of Cs diffusing across and through semiconductor coatings is undoubtedly more complex: existing evidence suggests, for example, that diffusion across metal surfaces proceeds more rapidly. Nevertheless, using a dispenser photocathode with such coatings will involve the migration of Cs through the diffusion barrier, and because experimental measurements of dispenser operation convolve migration through the barrier and diffusion across the surface, the latter must be well understood theoretically before measured constants for the former can be confidently inferred and applied to the semiconductor-coated dispenser case.

## 6. Alkali Antimonide Coatings

### 6.1. Fabrication of alkali antimonide cathodes at UMD

Building on previous results for the simplest cesium-based cathode, the binary cesiated tungsten system, we have added antimony and alkali metal deposition capabilities to our experimental apparatus. We have reported<sup>11</sup> the initial fabrication of a cesium antimonide ( $\text{Cs}_3\text{Sb}$ ) cathode with QE at 532 nm of 3.3% and at 375 nm of 11%. Our procedure for cathode fabrication for  $\text{Cs}_3\text{Sb}$  begins with an Ar ion cleaning of the surface. The cathode is heated to 130° C. A prescribed thickness of antimony (100 Å in this example) is deposited from the evaporative source at a rate of 0.2 Å/s. Subsequently, cesium is evaporated onto the cathode surface at 0.1–0.2 Å/s, with the cathode being allowed to begin to cool after the first approximately 100 Å is deposited. Cesium deposition is stopped when the QE peaks: for the example above, after approximately 500–800 Å. The highest-QE cathode achieved at UMD followed the fabrication behavior shown in Fig. 6, where heating was turned off after approximately 4 h and vacuum during the subsequent slow rise in QE was about 0.5 ntorr.

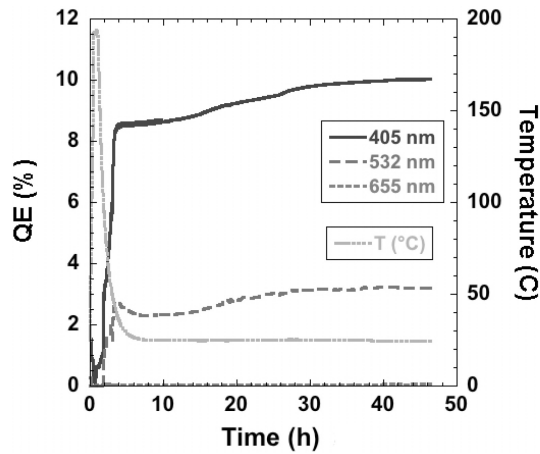


Fig. 6. Initial fabrication of high-QE Cs<sub>3</sub>Sb cathode, 100 Å initial Sb layer.

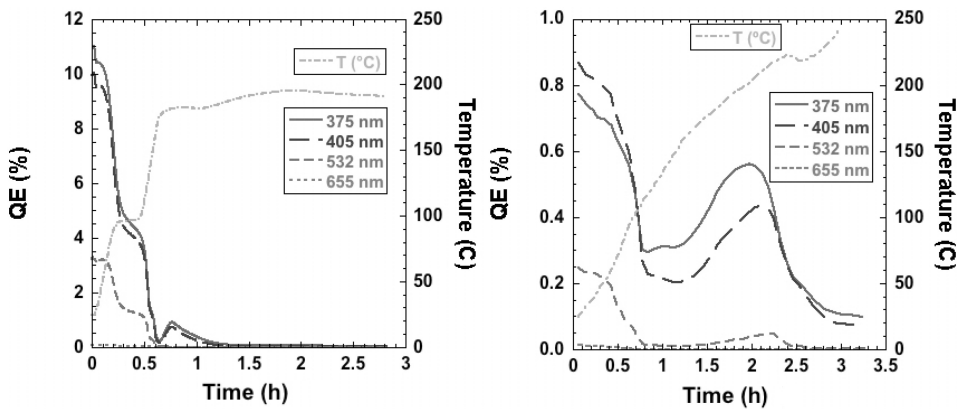


Fig. 7. Cs<sub>3</sub>Sb from initial 100-Å Sb layer (left) on porous W dispenser (without rejuvenation) versus that of an initial 41-Å Sb layer (right) on solid Ag.

6.2. Operating temperatures and coating compositions

As previously reported,<sup>11</sup> alkali antimonides can lose QE when heated. If the cathode is heated to less than a critical temperature and cooled again, the QE returns to previous levels. If the cathode is heated too much, the QE is irreversibly lost. The proposed loss mechanism is release and evaporation of alkalis, particularly cesium (which has the highest elemental vapor pressure), from the semiconductor compound. For cesium antimonide, the first alkali antimonide chosen for study in the UMD diagnostic chamber, some initial results of heating already-fabricated coatings are shown below. Cesium antimonide was chosen not because of its temperature stability (it is in fact less temperature stable than other alkali antimonides) but rather because it is more straightforward to fabricate, being a binary rather than ternary (K<sub>2</sub>CsSb) or more complex system. The time and temperature axes in Fig. 7 are of particular interest; the QE axis is not as important because the thicknesses of the coatings differ between the two tests. For a porous substrate, temperatures ramping to 200° C take

only about an hour to reduce QE to negligible levels. The similar experiment on a solid substrate shows a 3-h timescale, and a detailed investigation shall be reported separately. One possible explanation of the effect, however, is that cesium may diffuse into the porous material in the absence of any cesium resupply, simply following the concentration gradient when heated enough to have significant surface migration. In future dispensers this will be important so as to have a favorable concentration gradient for diffusion outward rather than inward. Nonetheless, the ability to initially achieve QE of 3% in the green on a porous substrate is an important demonstration toward a rejuvenated semiconductor dispenser photocathode.

### 6.3. Outlook for demonstrated rejuvenation of cesium-based semiconductor coatings

To demonstrate rejuvenation of cesium-based alkali-antimonide-coated dispenser photocathodes and an increased lifetime of such cathodes, three important capabilities must be clearly understood and achieved:

- repeatability of cathode QE using standardized fabrication procedures
- stability of cathodes under heating at temperatures sufficient for Cs migration from the reservoir through the diffusion barrier to the surface
- replacement of lost Cs in the surface coating and ensuing rejuvenation of QE at the aforementioned temperatures

The first task is nontrivial. The second involves a choice of cathode chemistry and impacts the first. Different cathode chemistries and layer compositions will have different temperatures at which they are stable. (It has been indicated that elevated temperature can, however, have a beneficial impact on cathode lifetime even without resupply of Cs from a dispenser or external source.<sup>3</sup>) Finally, the third task must satisfactorily show that at temperatures suitable for stability of the cathode layer and diffusion of Cs from the reservoir, the freely diffusing Cs can then reincorporate into the bulk of the coating or at least replace a surface layer in such a way as to benefit overall QE. This is not self-evident, and continuing experiments and modeling will probe the available parameter space in search of such a demonstration. The promise of a highly efficient, long-lived, prompt, and robust cathode should motivate progress toward these goals on both the experimental and theoretical fronts.

## 7. Acknowledgments

We gratefully acknowledge B. Vancil of E-beam, Inc., for dispenser cathode fabrication expertise and A. Balter of Oglethorpe University for cesiated silver and cesiated tungsten experiments and dispenser lifetime testing during the summers of 2005 and 2006 at UMD. We gratefully acknowledge funding provided by the Office of Naval Research and the Joint Technology Office.

## References

- <sup>1</sup>Alanissila, T., and S. Ying, *Prog. Surf. Sci.* **39**, 227 (1992).
- <sup>2</sup>di Bona, A., F. Sabary, S. Joly, P. Michelato, D. Sertore, C. Pagani, and S. Valeri, *Nucl. Instrum. Methods Phys. Res. A* **385**, 385 (1997).
- <sup>3</sup>Dowell, D. H., *Proc. SPIE* **3614**(1), 14 (1999).

- <sup>4</sup>Falce, L. R., and R. E. Thomas, *International Electron Devices Meeting* **24**, 156 (1978).
- <sup>5</sup>Green, M. C., *Technical Digest of the International Electron Devices Meeting* **26**, 471 (1980).
- <sup>6</sup>Jensen, K. L., D. W. Feldman, N. A. Moody, and P. G. O'Shea, *J. Appl. Phys.* **99**, 124905 (2006).
- <sup>7</sup>Jensen, K. L., D. W. Feldman, M. Virgo, and P. G. O'Shea, *Phys. Rev. ST Accel. Beams* **6**, (14) (2003).
- <sup>8</sup>Jensen, K. L., N. A. Moody, D. W. Feldman, E. J. Montgomery, and P. G. O'Shea, *J. Appl. Phys.* **102**, 074902 (2007).
- <sup>9</sup>Kong, S. H., J. Kinross-Wright, D. C. Nguyen, and R. L. Sheffield, *Nucl. Instrum. Methods Phys. Res. A* **358**, 272 (1995).
- <sup>10</sup>Michelato, P., *Nucl. Instrum. Methods Phys. Res. A* **393**, 455 (1997).
- <sup>11</sup>Montgomery, E. J., D. W. Feldman, P. G. O'Shea, Z. Pan, N. A. Moody, and K. L. Jensen, *Proc. PAC 2007 TUPMS010*, Albuquerque, NM, June 25–29, 2007; <http://accelconf.web.cern.ch/AccelConf/p07/>.
- <sup>12</sup>Moody, N. A., D. W. Feldman, E. J. Montgomery, A. E. Balter, P. G. O'Shea, K. L. Jensen, J. E. Yater, and J. L. Shaw, *Proceedings of FEL 2006*, 748, Berlin, Germany, August 27–September 1, 2006; <http://www.bessy.de/fel2006/>.
- <sup>13</sup>Moody, N. A., K. L. Jensen, D. W. Feldman, P. G. O'Shea, and E. J. Montgomery, *Appl. Phys. Lett.* **90**(11), 114108 (2007).
- <sup>14</sup>Moore, G. E., and H. W. Allison, *J. Chem. Phys.* **23**, 1609 (1955).
- <sup>15</sup>O'Shea, P., and H. Freund, *Science* **292**, 1853 (2001).
- <sup>16</sup>Rao, T., A. Burrill, X. Y. Chang, J. Smedley, T. Nishitani, C. Hernandez-Garcia, M. Poelker, E. Seddon, F. E. Hannon, C. K. Sinclair, J. Lewellen, and D. Feldman, *Nucl. Instrum. Methods Phys. Res. A* **557**(1), 124 (2006).
- <sup>17</sup>Reiser, M., *Theory and Design of Charged Particle Beams*, Wiley-Interscience, New York (1993).
- <sup>18</sup>Smith, G. D., *Numerical Solution of Partial Differential Equations: Finite Difference Methods*, Oxford University Press, New York (1985).
- <sup>19</sup>Sommer, A. H., *Photoemissive Materials*, Wiley, New York (1969).
- <sup>20</sup>Suberlucq, G., "Development and Production of Photocathodes for the CLIC Test Facility," *Proc. 18th International FEL Conference and Applications Workshop*, pp. 20–30, Rome, Italy, August 26–30, 1996.
- <sup>21</sup>Thomas, R. E., J. W. Gibson, G. A. Haas, and R. H. Abrams, Jr., *IEEE Trans. Electron. Devices* **37**, 850 (1990).
- <sup>22</sup>Veisfeld, N., and J. D. Geller, *J. Vac. Sci. Tech. A* **6**, 2077 (1988).

## The Authors

**Dr. Donald W. Feldman** is a Visiting Research Scientist at the University of Maryland. He received his Ph.D. in physics from UC Berkeley in 1959. He began his career at the Westinghouse Research Laboratory that same year. From 1985 until his retirement in 1993, he worked on free-electron lasers at the Los Alamos National Laboratory. Between 1993 and his present position at UMD, Dr. Feldman consulted for various organizations, such as CEA, Bruyeres-Le-Chatel in France, Northrop Grumman, and Los Alamos. His primary interests have been in research and development of gas lasers, free-electron lasers, and RF electron linacs and the application of RF, microwave, and optical spectroscopic techniques to the study of various solid-state and applied problems. More recently, his interests have been primarily in photoinjection processes in a low energy storage ring (UMER) and in the development of improved photocathodes for high-current photoinjectors. Dr. Feldman is the author and coauthor of more than 50 peer-reviewed papers and conference papers.

**Dr. Kevin L. Jensen** received the B.S. degree in applied physics from Columbia University, New York, in 1981, and the M.S. and Ph.D. degrees in physics from New York University, New York, in 1984 and 1987, respectively. In 1987, he joined the Naval Research Laboratory as an NRC post doc in the Semiconductors Branch of the Electronics Science and Technology Division (ESTD), for work on quantum transport in resonant tunneling diodes. In 1990, he became a member of the Vacuum Electronics Branch in ESTD, for theoretical work on emission properties of electron sources. He has authored and coauthored more than 104 journal articles, book chapters, and encyclopedia articles; coedited

three Proceedings volumes for the Materials Research Society and the Electrochemical Society on cold cathodes; was guest editor for the “Special Issue on Vacuum Microelectronics” in *Solid State Electronics* 45 (2001); and is on the conference committees of the International Vacuum Electron Sources Conference (IVESC) and the International Vacuum Nanoelectronics Conference (IVNC). He has recently written a book entitled *Electron Emission Physics* (Academic Press, 2007). His research interests are in quantum transport and electron emission physics in relation to RF vacuum electronics.

**Mr. Eric J. Montgomery** received the B.S. degree in physics and optical engineering from the University of Maryland, Baltimore County, in 2005, and the M.S. degree in physics from the University of Maryland, College Park, in 2008. He was a National Merit Scholar, Maryland Distinguished Scholar, and UMBC University Scholar as an undergraduate, graduating summa cum laude. As a graduate student, he has received a Directed Energy Professional Society (DEPS) fellowship, a first-year fellowship from the UMD Physics Department, and a three-year scholarship from the Institute for Research in Electronics and Applied Physics. He has received numerous speaking awards, most recently giving a plenary talk for Best Student Poster at the 2008 Advanced Accelerator Concepts Workshop. He has authored or coauthored six peer-reviewed journal articles and several conference proceedings. His current doctoral research at UMD is on the design and experimental development of high-quantum-efficiency dispenser photocathodes.

**Dr. Nathan A. Moody** received his B.S., M.S., and Ph.D. degrees in electrical engineering from the University of Maryland, College Park, in 2000, 2004, and 2006, respectively. He joined Los Alamos National Laboratory the same year as a Technical Staff Member and experimental task lead on LANL’s normal conducting radio frequency (NCRF) free-electron laser photoinjector program, where he oversaw installation and initial RF testing of the cavity structure and its subsystems. For his leadership in launching new programs, he received the 2007 Exceptional Service Award and is principal investigator for two other technically diverse programs related to directed energy. His most recent effort involves design and fabrication of THz sources and compatible components using novel engineered materials and superconducting thin films. His ongoing work on electron source development has helped lay the foundation for a leading cathode technology (alkali dispenser photocathode), and he now serves as Chief Scientist of the NCRF photoinjector program.

**Dr. Patrick G. O’Shea** is Chair of the Department of Electrical & Computer Engineering and former Director of the Institute for Research in Electronics and Applied Physics at the University of Maryland. He received his Ph.D. degree in physics from the University of Maryland. His early research was at Los Alamos National Laboratory, first on the Beam Experiment Aboard Rocket Project (1986–1990), which studied the propagation of beams in the Earth’s magnetosphere. In 1990, he was appointed Project Leader of the LANL Free Electron Laser Project, where he led the team that built and operated the first RF photoinjector linear accelerator and the first linear-accelerator-driven ultraviolet FEL. From 1994 to 1998 he was at Duke University, where he led the construction of the 300-MeV photoinjector linear accelerator. He is a Fellow of the American Physical Society, the Institute for Electrical and Electronics Engineers, and the American Association for the Advancement of Science.

**Mr. Peter (Zhigang) Pan** received his B.S. in physics from the University of Maryland, Baltimore County (UMBC), in 2007, where he was a Meyerhoff Scholar, graduating magna cum laude. He is currently in the Ph.D. program in physics at the University of Maryland, College Park (UMD). His research interests are in the theory and modeling of alkali dispenser photocathodes in support of experimental work ongoing at UMD. He was the

winner of the Best Speaker Award for the 2007 TREND summer research program at UMD, presented his research at the 2008 Advanced Accelerator Concepts Workshop, and has been author or coauthor on three publications.

**Mr. Noah Sennett** is a student in the science magnet program at Montgomery Blair High School (MBHS) in Montgomery County, Maryland. He was a 2008 National Merit Finalist, a 2008 recipient of the Maryland Governor's Merit Scholastic Award, and a semifinalist for the 2008 U.S. Physics Team to go to the International Science Olympiad. In 2006–2007 he served as his class president at MBHS. He worked with the Photocathode Research Laboratory at the University of Maryland, College Park, during summer 2007 with a research focus on the automated measurement of the quantum efficiency of dispenser photocathodes.